

Light-field modulation and optimization near metal nanostructures utilizing spatial light modulators

Zini Cao(曹子倪), Hai Lin(林海), Yuqing Cheng(程宇清), Yixuan Xu(徐艺轩), Qihuang Gong(龚旗煌), and Guowei Lü(吕国伟)

Citation: Chin. Phys. B, 2024, 33 (**10**): 104201. DOI: 10.1088/1674-1056/ad6555
Journal homepage: http://cpb.iphy.ac.cn; http://iopscience.iop.org/cpb

What follows is a list of articles you may be interested in

Surface phonon resonance: A new mechanism for enhancing photonic spin Hall effect and refractive index sensor

Jie Cheng(程杰), Chenglong Wang(汪承龙), Yiming Li(李一铭), Yalin Zhang(张亚林), Shengli Liu(刘胜利), and Peng Dong(董鹏)

Chin. Phys. B, 2024, 33 (**8**): 084201. DOI: 10.1088/1674-1056/ad4a3c

Tunable artificial plasmonic nanolaser with wide spectrum emission operating at room temperature

Peng Zhou(周鹏), Jia-Qi Guo(郭佳琦), Kun Liang(梁琨), Lei Jin(金磊), Xiong-Yu Liang(梁熊玉), Jun-Qiang Li(李俊强), Xu-Yan Deng(邓绪彦), Jian-Yu Qin(秦建宇), Jia-Sen Zhang(张家森), and Li Yu(于丽)

Chin. Phys. B, 2024, 33 (**5**): 054210. DOI: 10.1088/1674-1056/ad2dca

Giant and controllable Goos—Hänchen shift of a reflective beam off a hyperbolic metasurface of polar crystals

Tian Xue(薛天), Yu-Bo Li(李宇博), Hao-Yuan Song(宋浩元), Xiang-Guang Wang(王相光), Qiang Zhang(张强), Shu-Fang Fu(付淑芳), Sheng Zhou(周胜), and Xuan-Zhang Wang(王选章)

Chin. Phys. B, 2024, 33 (**1**): 014207. DOI: 10.1088/1674-1056/acdac2

Enhanced and controllable reflected group delay based on Tamm surface plasmons with Dirac semimetals

Qiwen Zheng(郑棋文), Wenguang Lu(卢文广), Jiaqing Xu(胥加青),Yunyang Ye(叶云洋), Xinmin Zhao(赵新民), and Leyong Jiang(蒋乐勇)

Chin. Phys. B, 2023, 32 (**7**): 074208. DOI: 10.1088/1674-1056/aca205

Simultaneous measurements of refractive index and temperature based on a no-core fiber coated with Ag and PDMS films

Yuxin Li(李宇昕), Hailiang Chen(陈海良), Yingyue Zhang(张赢月), Qiang Chen(陈强), Biao Wu(武彪),Xiaoya Fan(樊晓亚), Yingchao Liu(刘英超), and Mingjian Ma(马明建)

Chin. Phys. B, 2023, 32 (**5**): 054209. DOI: 10.1088/1674-1056/ac8f36

TOPICAL REVIEW — Optical field manipulation

Light-field modulation and optimization near metal nanostructures utilizing spatial light modulators

Zini Cao(曹子倪)[1], Hai Lin(林海)[1], Yuqing Cheng(程宇清)[2], Yixuan Xu(徐艺轩)[1], Qihuang Gong(龚旗煌)[1,3,4], and Guowei Lü(吕国伟)[1,3,4,†]

[1] *State Key Laboratory for Mesoscopic Physics, Collaborative Innovation Center of Quantum Matter, Frontiers Science Center for Nano-Optoelectronics, School of Physics, Peking University, Beijing* 100871, *China*
[2] *School of Mathematics and Physics, University of Science and Technology Beijing, Beijing* 100083, *China*
[3] *Collaborative Innovation Center of Extreme Optics, Shanxi University, Taiyuan* 030006, *China*
[4] *Peking University Yangtze Delta Institute of Optoelectronics, Nantong* 226010, *China*

(Received 20 April 2024; revised manuscript received 12 July 2024; accepted manuscript online 19 July 2024)

Plasmonic modes within metal nanostructures play a pivotal role in various nanophotonic applications. However, a significant challenge arises from the fixed shapes of nanostructures post-fabrication, resulting in limited modes under ordinary illumination. A promising solution lies in far-field control facilitated by spatial light modulators (SLMs), which enable on-site, real-time, and non-destructive manipulation of plasmon excitation. Through the robust modulation of the incident light using SLMs, this approach enables the generation, optimization, and dynamic control of surface plasmon polariton (SPP) and localized surface plasmon (LSP) modes. The versatility of this technique introduces a rich array of tunable degrees of freedom to plasmon-enhanced spectroscopy, offering novel approaches for signal optimization and functional expansion in this field. This paper provides a comprehensive review of the generation and modulation of SPP and LSP modes through far-field control with SLMs and highlights the diverse applications of this optical technology in plasmon-enhanced spectroscopy.

Keywords: surface plasmon, spatial light modulator, dynamic control, plasmon-enhanced spectroscopy

PACS: 42.40.Eq, 73.20.Mf, 78.67.Bf, 95.75.Qr **DOI:** 10.1088/1674-1056/ad6555

1. Introduction

The advancements in nanofabrication technology have paved the way for investigating optical phenomena at subwavelength scales, thus facilitating the development of compact, miniature, and integrated optical devices. Nevertheless, overcoming the diffraction limit of light remains an enormous challenge in nano-optics research and integrated optics applications. Surface plasmons (SPs)[1–3] have attracted substantial interest owing to their potential for breaking this limitation. SPs represent surface waves that emerge at interfaces between materials with negative dielectric constants and dielectrics through collective electron excitations accompanied by electromagnetic fields. Perpendicular to these interfaces, SPs demonstrate exponentially decaying evanescent fields and effectively confine the light field within subwavelength scales.

Due to the interaction between light and electrons, SPs exhibit distinctive optical properties, including confinement of the optical field at the metal–dielectric interface on a subwavelength scale and significant enhancement in the near-field.[4] The localization property enables SPs to overcome the diffraction limit. Optical signals can be transmitted and manipulated with ultra-high spatial resolution. Simultaneously, the near-field enhancement characteristic effectively amplifies inherently weak interactions between light and matter,[5] enhancing both efficiency and sensitivity in optical detection. These properties provide SPs with extensive potential for advancement across various disciplines such as physics,[6,7] chemistry,[8] and biology,[9] as well as diverse applications involving plasmonics like surface plasmon resonance sensing,[10] plasmon microscopy,[11] plasmonic optical communication,[12] surface-enhanced Raman scattering (SERS)[13] and surface-enhanced fluorescence.[14]

To harness robust field localization and near-field enhancement capabilities in various practical applications, it is often imperative to excite customized plasmon modes to achieve specific functionality. A typical example of a plasmon application is SERS, which utilizes gaps in disordered metal films.[15,16] Bowtie nanoantenna dimers show significantly strong localized fields to enhance a single molecule's fluorescence.[17] In addition, the excitation of unique SP modes (e.g., SP standing waves[18,19]) can facilitate super-resolution imaging. Exciting and manipulating plasmonic modes are crucial for innovative plasmonic devices and the ongoing discovery of plasmonic properties. A common approach is to design the geometry of nanostructures to support different plasmonic modes. The intrinsic modes of these nanostructures are determined by their structures,[3] and thus,

[†]Corresponding author. E-mail: guowei.lu@pku.edu.cn

© 2024 Chinese Physical Society and IOP Publishing Ltd

specific plasmonic modes can be designed and excited by varying the shape, size, arrangement, and composition of the nanostructures. For example, metal nanoparticles[20,21] of various shapes, such as nanorods, and metasurfaces[22] of various functionalities can support different SP modes.

However, these nanostructures typically exhibit a fixed shape after fabrication, leading to immutable intrinsic modes. It presents a challenge in actively controlling the plasmon modes. Despite the unalterable geometry of nanostructures, manipulating various degrees of freedom associated with the incident light is still feasible to excite and modulate the plasmon modes. This provides an opportunity for achieving active control over plasmon modes by tuning specific parameters of the incident light on a given nanostructure. Numerous studies have demonstrated that dynamic control of excited plasmonic modes can be attained by manipulating polarization,[23–25] wavelength,[26] wavefront phase,[27] wavevector direction, and other degrees of freedom associated with the incident light.

Spatial light modulators (SLMs)[28,29] are powerful tools, which are versatile enough to manipulate many different aspects of free-space light. Commercial spatial light modulators[29] mainly include liquid crystal spatial light modulators (LC-SLMs)[30,31] and digital micromirror devices (DMDs),[32] differing in their working principles. LC-SLM can generate phase holograms by electrically modulating the liquid crystal molecular orientation, while DMD can generate binary amplitude holograms by electromechanically controlling the spatial orientation of highly reflective micromirrors. In this context, both LC-SLMs and DMDs are referred to as SLMs. By utilizing pixel electrodes based on complementary metal–oxide–semiconductor (CMOS) technology, SLMs possess a large number of controllable pixel elements with micrometer scales and precise modulation capabilities. This enables them to generate high-resolution digital holograms in real time for modulating free-space light.

Empowered by highly controllable and encodable digital holograms, SLMs have a powerful and convenient modulation capability. Almost any desired light field can be created by SLMs.[33] In terms of shaping the wavefronts of continuous light, wavefronts with arbitrary phase and amplitude distributions can be realized by a two-step modulation strategy, even though conventionally LC-SLMs modulate only the phase and DMDs modulate only the amplitude. For example, phase-type digital holograms generated by an LC-SLM can be used to modulate the phase of free-space light firstly, and then spatially filtered in a $4f$ system. The two-step strategy will ultimately realize simultaneous modulation of the phase and amplitude distributions of the free-space light wavefront. To generate optical wavefronts with specific characteristics, such as convergent spherical waves with customizable focus positions,[34] Laguerre–Gaussian beams,[35–38] vortex beams,[39] non-diffracting beams[40–42] and flat-top beams, wavefront shaping has been widely used. In addition, polarization control in shaped wavefront shaping may be achieved by separately modulating different polarization components of the beam. For example, separating the beam into two orthogonally polarized components using a polarizing beam splitter (PBS), modulating each component with an SLM-based wavefront shaping path, and then recombining them. Polarization-controlled wavefront can produce a more complex vector beam, such as a vectorial vortex beam.[43–45] In terms of shaping pulsed light, elements such as gratings or prisms can be used to spatially separate the different frequency components of the pulse, which can then be controlled using different regions of the SLM.

The research field of generating arbitrary wavefronts using SLMs combined with specially designed nanostructures of specialized designs is promising. Wavefront shaping can actively control various properties of light, such as phase, amplitude, polarization, and other degrees of freedom, thus implementing the excitation and manipulation of SP modes with specific properties using SLMs. By shaping free-space light using SLMs, the flexibility allows the generation of customized free-space light fields to customize and control SP modes.

This review aims to introduce the modulation of SP modes using SLMs and its applications in plasmon-enhanced spectroscopy. Section 2 offers a concise overview of the properties of propagating SP modes and surface plasmon polaritons (SPPs) and the challenges and methods involved in exciting and controlling these plasmonic modes through modulation of the incident light using SLMs. Section 3 discusses techniques for selectively exciting hotspots of localized surface plasmon (LSP) modes as well as their applications and dynamic control. Section 4 presents improved approaches for the conventional plasmon-enhanced spectroscopy by modulating the generated plasmonic modes using SLMs. Finally, we summarize the research on combining SLMs with SP modes and provide insights into future developments. It is important to note that this paper focuses specifically on the excitation of plasmonic modes using structured light generated by SLMs, while other topics, such as SLMs based on SP resonance principles[46] or manipulation of metal nanoparticles using structured light optical tweezers generated by SLMs[47–49] are beyond the scope of this paper. Interested readers are encouraged to refer to related articles for further information.

2. Wavefront design and modulation of SPP

The properties of SP enable localizing optical field and near-field enhancement, greatly facilitating light–matter interactions. Metal nanostructures have facilitated the study of

the design and control of specific SP modes, laying the foundation for various applications based on SP devices. These modes provide key methods for directing and enhancing optical signals at the nanoscale, thus opening up new possibilities in nano-optical applications.

At the interface of metal and dielectric materials, an intensively localized light excitation mode known as SPP emerges.[50] The evanescent field of SPP decays exponentially in both directions perpendicular to the interface, and it diminishes substantially smaller than the wavelength in free space. This highly localized effect allows the propagation of SPP to be modeled using a two-dimensional Helmholtz equation, manifesting itself as a two-dimensional electromagnetic mode. This concept not only simplifies the understanding of the physical properties of SPP but also provides innovative strategies for controlling SPP modes reliant on expertise in light manipulation. The properties of the SP mode in the plasmonic waveguide depend on the geometric configuration of the nanostructure. The behavior of SP mode can be controlled by fabricating precise nanostructure waveguides,[51] like etched flat metal waveguides, modulating the dielectric refractive index of the surface, and constructing nanowires. Besides the propagating SPP modes, LSP has also gained considerable attention.[52] The LSP modes confine light within specific regions, leading to highly intensified light fields and significantly enhancing the interaction between light and matter. The LSP modes are widely employed in spectroscopy signal enhancement, highlighting the practical applicability of these modes.

Direct excitation of SPP modes with free-space light is infeasible due to the mismatch between the wave vectors. Therefore, specific coupling structures are required to ensure wave vector matching. These structures could be achieved using prism, scattering, and grating coupling.[50] The excited SPP wavefront is generated through the interference of contributions from each cell in the coupling structure. Thus, even a slight variation in the contribution of each cell can induce a change in the SPP wavefront. Designing the geometric phase of the coupling structures influences the excitation of SPP modes,[24] and studies have shown that specific SPP wavefronts can be efficiently excited and controlled by carefully designing these structures. Similarly, modulation of SPP modes can be achieved by directly modulating the polarization, wavevector frequency, and other characteristics of the incident light to change the excitation modes of the units of the coupling structure. Compared with the complex design and fixed coupling structure, the design and dynamic modulation of a specific SPP wavefront can be realized by modulating multiple degrees of freedom of the incident light wavefront, thus providing a powerful method to control the SPP modes actively.

2.1. SPP focus

Light focusing is the convergence of a light beam into a smaller spatial region. In classical optics, optical focusing is achieved by a lens providing a quadratic phase factor to the free-space optical wavefront so that the wavefront is approximated as a converging spherical wave and converges at a point in space. This concentration of the light field energy in space is integral to enhancing microscopic resolution, interactions between light and matter, information storage density, and information communication speed. Similarly, according to the two-dimensional Helmholtz equation, an SPP wavefront with a given phase and amplitude distribution exhibits a unique propagation pattern. Specific SPP wavefronts can be generated by appropriate techniques involving SLM-shaped wavefronts. Dynamic and flexible alteration of the incident beam can generate and manipulate various SPP focusing modes as required. It is a convenient strategy for overcoming the limitations of fixed lenses or nanostructures. Moreover, shaped wavefront profiles can also improve SPP focusing by increasing coupling efficiency and tunability, resulting in high-quality SPP focusing.

Light with converging wavefronts can focus on one position (or several positions), such as converging spherical waves, plane waves passing through the Fresnel zone plate, and so on. Both the design of coupling structures and modulation of excitation light can be informed by knowing the 2D converging wavefront patterns. These strategies enable the generation of converging SPP wavefronts, which are like converging cylindrical waves in free space, and then lead to SPP focusing on the desired positions.[53,54,58] Zhao *et al.*[53] demonstrated dynamic control of SPP focus. By using an SLM to generate 2D Fresnel-zone type SPP patterns on a metal film with a coupling grating, they could dynamically control the position of the focused SPP spot both in parallel and perpendicular directions. The results were confirmed by leakage radiation microscopy. They suggested that the method could be helpful for various plasmonic applications. A similar method is the phase-controlled excitation light wavefront mode. It can alternatively be employed for the focusing and dynamic manipulation of the SPP focus position. Yuan *et al.*[58] demonstrated that by using a SLM to generate vortex light with different topological charges and irradiating them on a metal film with an arc-shaped slit, they could dynamically control the position and shape of the focused SPP spot on the metal surface. They confirmed their results by using finite-difference time-domain simulations and near-field scanning optical microscopy measurements.[54]

As illustrated in the previous SPP focusing examples about achieving SPP focusing and required spatial positioning, the design of excitation light wavefront modes exhibits great

flexibility. This flexibility suggests that the light wavefront modulated by an SLM offers a vast range of options for optimizing the focusing mode.[55,59–61] For example, it is possible to target the focus of SPP onto any specific spatial position. Gjonaj *et al.*[55] demonstrated that using an SLM to modulate the incident light amplitude and phase on a metal film with a nanohole array, they could dynamically control the position and shape of the focused SPP spot on the metal surface. They confirmed their results using numerical simulations and near-field scanning optical microscopy measurements. In their interpretation, SPP focusing idealizes a superpixel into a light source placed at a specific location in the illumination area. When all sources contribute phases consistently at the target position, the target field reaches a peak value, thus leading to SPP focusing. The highly symmetrical periodic nanopore array featured in this study allows for theoretical calculations and analyses. Therefore, they use the measured Green function to link the input of the excited light to the single-point SPP complex amplitude output. The measured Green function is adaptable to the creation of SPP modes based on any arbitrary nanostructure and any field distribution. Subsequently, Gjonaj *et al.*[59] have showcased Bloch mode-altered SPP in arrays of nanoholes with varying sub-wavelength periodicities. A counter-propagating SPP interference pattern is generated, enabling precise manipulation of the pattern's translation and orientation by modulating the phase of superpixels. As the SPP wavelength is smaller than that of free-space light, superior optical diffraction resolution is achievable by designing nanostructure lenses to decrease the numerical aperture of SPP. Based on this principle, 2D scanning imaging plasmon microscopy has been accomplished by generating an SPP focal point with the phase-structured illumination of an SLM.[60]

A comprehensive understanding of their SPP mode excitation and propagation for simple nanostructures can improve SPP functionality. The SPP wavefront intensity and phase at specific locations are determined by merging theoretical and numerical computations to guide the excitation light wavefront phase configuration. Understanding the relationship between the excitation light wavefront phase and SPP focal point position permits the acquisition of any given intensity distribution pattern.[56,62] Wei *et al.*[56] demonstrated that by using an SLM to modulate the phase of the incident light on a metal film with a ring slit, they could dynamically control the position and shape of the focused SPP spot on the metal surface. They confirmed their results using numerical simulations and near-field scanning optical microscopy measurements. This methodology can generate broadband SPP modes, delivering potential applications for creating different frequency SPP fields, high-speed in-plane communication, and high data storage capacity.

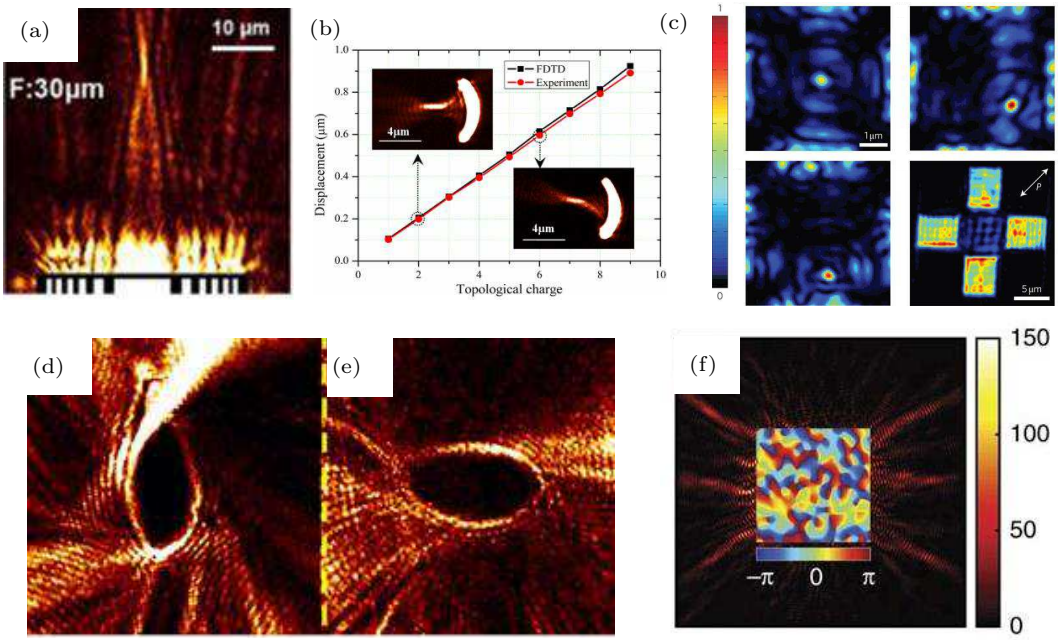


Fig. 1. Dynamic focusing of SPPs through (a) amplitude modulation of a Fresnel-zone type beam incident on a grating coupler.[53] SPP patterns with Fresnel-zone type binary wavefront on the Au film focused at the point determined by the order number of Fresnel zone. (b) Phase modulation of an optical vortex beam incident on an arc-slit-shaped nanostructure.[54] The figure shows the vertical displacement of the SPP focal spot versus the topological charge of the optical vortex beam. The insets show near-field intensity distributions for topological charges of 2 (upper left) and 6 (lower right). (c) Shaped wavefront designed by Green function.[55] The lower right picture shows a background reference of a uniform phase profile wavefront, and the other pictures show that SPPs focus on freely chosen targets. (d)–(e) Shaped wavefront designed by numerical computations of phase retrieval algorithm.[56] Intensity distributions of elliptically shaped intensity patterns with different eccentricities and orientations. (f) Shaped wavefront designed by the measured transfer matrix.[57] The picture shows that SPP focused on 6 points, measured by a leakage radiation microscope.

The ordered symmetries of periodic nanostructures may trigger a decoupling from specified free-space optical modes. The decoupling decreases the practical degrees of freedom in wavefront control. Hence, using disordered nanostructures is advantageous due to their capability to enhance the signal intensity of input and output channels. Historical complexities associated with disordered structures have limited research and applications. However, the strong wavefront control capacity of the SLM has uncovered and employed the transmission characteristics of disordered media.[57,63,64] Utilizing SLM to reveal disordered input and output properties of nanostructures is essential for exploiting these structures, and then their unique wavefront modes produced and customized via SPP modes. Making use of the flexibility of SLMs, it is helpful to acquire the transmission matrix of nanostructures. Choi *et al.*[57] demonstrated that by using an SLM to modulate the wavefront of the incident light on a metal film with a disordered nanopore array, they could dynamically control the position and shape of the focused SPP spot on the metal surface. They confirmed their results using numerical simulations and near-field scanning optical microscopy measurements. Their method could be helpful in various plasmonic applications. This breakthrough significantly increases the input–output channel relationship from far-field to SPP, promoting the application of SPP in optoelectronic devices.

2.2. SPP and orbital angular momentum

Light can carry both spin angular momentum (SAM) and orbital angular momentum (OAM). The former corresponds to circular polarization, and the latter is associated with the spiral phase of the wavefront.[65] It was revealed by Allen *et al.* in 1992 that there is an intrinsic correlation between the spiral phase wavefront and OAM of light. A direct correspondence is between the topological charge of the phase singularity of the spiral phase and the quantum state of the quantized OAM of photons. The pioneering work by Allen *et al.* points out the unique topological properties of OAM beams, thus giving rise to a tunable degree of freedom that has been exploited in diverse fields, such as optical tweezers, imaging and microscopy, quantum optics, and optical communication.

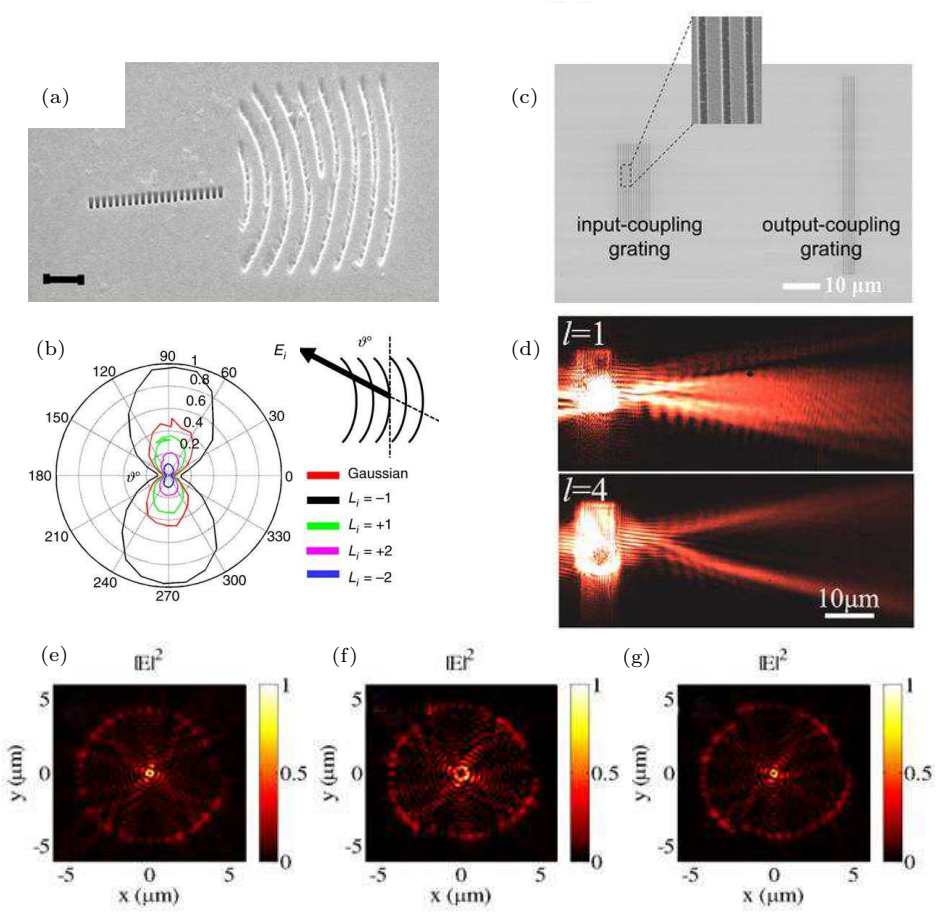


Fig. 2. (a)–(b) Holographic SPP coupler for detecting vortex light with a specific topological charge.[66] (a) Scanning electron micrograph image of the holographic coupler, scale bar 1 μm. (b) Photocurrent measurements of the photodiode show that the maximum photocurrent is measured for vortex light with a topological charge of −1. (c), (d) SPP grating coupler for detecting the topological charge of an arbitrary vortex beam.[67] (c) SEM image of the grating coupler with a scale bar of 10 μm. (d) Different vortex beams have different beam splitting angles determined by the topological charge, and quantitative measurements of the topological charge can be realized based on the splitting angle. (e)–(g) Simulation results of plasmonic vortex beams produced by Archimedean helical plasmonic lens.[68] The figure shows the plasmon vortex beams with different topological charge l, helical structure geometric charge m, and circular polarization parameter s, where (e) $(l,m,s) = (0,1,0)$, (f) $(l,m,s) = (0,3,0)$, and (g) $(l,m,s) = (-1,3,-1)$.

Employing nanostructures as couplers enables the coupling of vortex light to specific SPP modes. An SLM is an effective tool to generate vortex light with varying topological charges and is extensively employed in related studies.[66,67,69] Genevet *et al.*[66] developed a plasmon coupler based on a holographic surface that could selectively couple vortex light with a specific topological charge to a focused SPP mode, thus enabling the detection of vortex light with different topological charges. Chen *et al.*[67] devised a compound grating that could couple vortex light with different topological charges to SPP modes with different propagation directions, enabling the routing of vortex light with different topological charges.

In contrast to free-space light, SPPs offer superior optical field confinement and subwavelength characteristics, thereby potentially expanding the application of vortex light into the nanometer scale. An SPP mode carrying OAM is known as plasmon vortex light. The spiral phase of the exciting light can produce plasmon vortices through a coupling structure that excites the SPP wavefront with the spiral phase. It has been empirically verified that plasmon vortices can be elicited by devising the geometric phase of the coupling structure, such as spiral structures and metasurfaces. It implies the feasibility of dynamic control of plasmon vortices by varying the topological charge and spin of the incident vortex light. These plasmon lens structures, known as coupling structures, often exhibit distinct responses to excitation light with varying topological charges and spins, such as selectively inducing plasmon vortices with dissimilar topological charges or altering the central position of the plasmon vortex.[68]

2.3. SPP non-diffraction beams

The three-dimensional Helmholtz equation determines the phenomenon of light propagation in free space. The wave characteristics of light induce diffraction phenomena during propagation, which consequently cause alterations in the phase front amplitude. A breakthrough occurred in 1987 when Durnin could mathematically determine a specific Bessel beam resolution to the Helmholtz equation that remains unaltered throughout its propagation.[70] Intensely scrutinized for its unique, consistent wavefront and non-diffracting properties, this light travels in a linear path. In addition, self-accelerating beams, or curved-line propagation solutions, successfully preserving constant wavefronts, were identified. This concept was named thus due to the prediction of Berry and Balazs surrounding the unique 'acceleration' properties of Airy wave packets in free space, despite no external forces acting upon them.[71] Siviloglou suggested an innovative approach in 2007 to truncate infinitely energetic Airy beams.[72] This technique successfully created Airy beams propagating in a parabolic trajectory during experimental trials, attracting significant interest. The research scope quickly extended to Airy beams with arbitrarily defined convex trajectories and beyond to Bessel and Mathieu beams with arbitrary convex trajectories.

The propagation of SPPs satisfies the two-dimensional Helmholtz equation. Unlike the free-space light, which is three-dimensional, only two non-diffracting solutions under paraxial approximation are available for monochromatic SPP: plane wave and Airy beam.[71] Plane waves are diffraction-free, and a consine beam which is the superposition of two mirror-symmetric plane waves is also diffraction-free. The cosine-Gauss surface plasmon beam, which is obtained from the interference of two Gaussian-envelope truncated SPP beams, has a narrow main lobe of SPP wavelength magnitude and self-healing characteristics. It was produced experimentally by dual grating couplers and achieved tunable propagation direction.[75,76] By adjusting the phase of the excitation light wavefront to replace the geometric phase provided by the angle of the grating couplers, SLM is beneficial for designing grating coupler structures as it can invoke linear phase modulation on the incident light. This allows reliable and simple excitation of SPP plane waves with varying wave vector directions. Wang *et al.* calculated a cosine-Gauss surface plasmon beam upon a gold film surface and a simplistic grating structure on a silica substrate.[73] By modulating the wavefront of the transmitted wave with the phase mask loaded on the SLM, it is demonstrated that the generation and the propagation direction modulation of the cosine-Gauss surface plasmon beam can be achieved by changing the phase mask. This reveals the feasibility of convenient generation and dynamic control of Gaussian cosine SPP beams through SLM.

The plasmonic Airy beam is the only non-trivial, non-diffracting solution to the two-dimensional Helmholtz equation under the paraxial approximation. The Airy beam propagates non-diffractively along a parabolic curve trajectory and exhibits self-healing properties. Plasmonic Airy beam has been demonstrated that its main lobe maintains the size and intensity better than SPP with a Gaussian envelope does.[77] In order to generate a plasmonic Airy beam, a specially designed grating coupler structure[78] or scattering structure[79] is required to obtain the wavefront phase of the Airy function distribution. Despite the strong energy dissipation on the metal surface, plasmonic Airy beam was still achieved experimentally. An alternative method is to use a free Airy beam generated by SLM, which is incident on a simple grating coupler to generate a plasmonic Airy beam. Zhang *et al.*[74] achieved generation and dynamic control generation of the surface plasmon Airy beam by modulating the wavefront of the incident light as it excited the grating coupling structure by wavefront shaping. They validated its light intensity as it propagated non-diffracting along a parabola through observation via a leakage radiation microscope. Moreover, they managed to showcase

real-time alterations in beam tilt angle via the computer addressing of the SLM, which effectively demonstrated the dynamic control of the surface plasmon Airy beam.

3. Selective excitation and dynamic control of LSP hotspots

At the sharp edges of metal nanostructures, gaps, and other geometries with nanometer fluctuation, localized surface plasmon can generate highly localized electromagnetic fields at the nanoscale known as hotspots. In the past decades, hotspots have been one of the critical drivers of nanoscale fabrication methods as well as the exploration of new materials for nanophotonics. As a considerable energy concentration mode, it was first discovered on rough metal surfaces.[15] Research interest has since expanded to include metal nanoparticles[20] of various shapes as well as metasurfaces[22] of various functionalities.

3.1. By pulse shaping

Before electron scattering resulted in decreased conductivity and the significant impact of electron tunneling on metal losses, there was a tendency for enhanced hotspot energy concentration in nanostructures as nanoparticle sharpness or interparticle gap distances reduced.[80] This has led to extensive research on metal nanoparticles with subwavelength dimensions in one or more directions. For simple metal nanoparticle structures, such as nanospheres and nanorods, the matching wavevector provided by the structure allows hotspots to be excited directly by free-space light. However, the excitation light wavefront felt by metal nanoparticles is limited by the diffraction limit in the subwavelength scale region. And the intensity and phase of excitation light remain almost at the same level. These reasons make it difficult to dynamically control the hotspot by modulating the phase of the incident light.

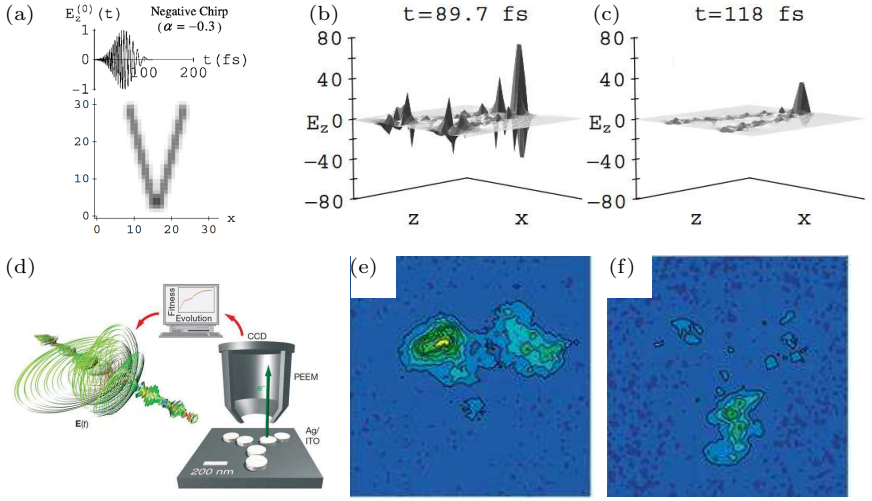


Fig. 3. Selective excitation and dynamic control of hotspots (a)–(c) by an ultrashort chirped pulse.[87] (a) Spatial distribution of the smooth density of the V-shaped nanostructure (lower) and the negatively chirped pulse (upper). (b) and (c) Simulation results of the spatial distribution of the localized electric field at different moments show that the excitation energy is concentrated at the apex of the V-shape during that period. (d)–(f) By adaptively shaped pulses.[88] (d) Schematic diagram of the experimental scheme for adaptive pulse shaping. (e) and (f) PEEM image of the hotspot after performing adaptive optimization, with emission dominating in the upper region and emission dominating in the lower region.

Metal nanostructures have frequency-dependent optical responses due to the intrinsic dielectric function dispersion of the material. Thus, the spatial distributions of modes generated by incident light excitation at different frequencies differ.[81] Based on the idea of coherent control,[82] the hotspot excitation can be effectively modulated. By using the different frequency components that ultrashort pulses have, appropriately modulating the intensities and phases of different frequency plasmon modes of coherent excitation can be realized.

Assuming that an ultrashort pulse is incident on the metal nanostructure, the different SP eigenmodes of the metal nanostructure will be excited by the pulse. And then the amplitude and phase of each frequency component of the pulse determine the intensity and phase of their excitation. If the total duration of the ultrashort pulse is smaller than the SP decoherence time, the different frequency-excited SP eigenmodes will coexist simultaneously. SP eigenmodes interfere in the overlapping region of time and space distribution.[83] By appropriate control of the intensity and phase of the excited SP eigenmodes, the SP modes at the desired position can constructively interfere at a given time. It will result in a high concentration of light field energy.

Coherent control based on the shaped pulse was earlier applied to control quantum states of atomic and molecular systems with microscopic chemical reaction processes.[84] Subsequently, optimization of the spectral phase of femtosecond laser pulses in combination with an iterative algorithm-controlled SLM pixel voltage-encoded pulse shaper was developed. It has been successfully applied to adaptive, coherent control of various types of chemical reactions. The coherent

control adaptive optimization does not depend on the information of the sample substance and has good scalability. The method is soon extended to the study of high harmonics[85] and nonlinear Raman spectroscopy.[86]

The concept of coherent control of ultrashort pulses can be naturally introduced to plasmonic excitation systems to achieve dynamic control of hotspots. Using phase modulation of femtosecond pulses as a functional degree of freedom, it is available to coherently control the plasmon excitation modes. Both the spatial distribution and concentration of energy of the plasmon can be designed. Stockman *et al.*[87] proposed the concept of coherent control in nanostructures. Theoretical calculation shows that the selective excitation of the given hotspots in nanostructures can be achieved by modulation of the chirp of the ultrashort pulse. Chirped pulses with Gaussian envelopes are considered for the excitation of V-shaped metal nanostructures. The simulation results show that a suitable negative chirp pulse drive can concentrate the excitation energy at the apex of the V-shape. It reveals the important role of phase modulation in the realization of spatially distributed dynamic modulation of local field of the nanostructures.

Ultrashort pulse chirped linear modulation can be extended to arbitrary phase difference modulation with the help of SLM pulse shaping. By making use of multiparameter-shaped pulses, achieving coherent control of plasmon excitation modes has been proven possible and powerful.[88–92] Aeschlimann *et al.*[88] used an adaptive algorithm to optimize a vast number of degrees of freedom of pulse shaping. They regulated the polarization state of the excitation pulses, which concerned the phase difference of the different frequency components. They achieved an adaptive polarization selective excitation control experimental results of the hotspot of nanostructures with the near-field distribution. The experiment employed a star-shaped arm structure composed of three silver-plate dimers with the nanogap of the silver-plate dimer disk supporting the hotspot mode. The excitation pulses, which were injected into the star-arm metal nanostructures, were modulated by the SLM pulse shaper. The intensity, instantaneous oscillation frequency, and polarization state were modulated. The high spatial resolution two-photon PEEM was used to measure the spatial distribution of the optical field intensity within the nanostructures, which provided feedback signals for the adaptive algorithm to implement the adaptive optimization of SLM pulse shaping. Thus, the dimer gaps of the different sub-wavelength regions could be successfully and selectively excited.

3.2. By wavefront shaping

Due to the continuous progress of nanofabrication technology, metasurfaces designed based on various complex structures can have many advantages, such as high efficiency, wide spectral bands, and low-cost fabrication, which has caused a boom in research on metasurfaces. Intercomponent interaction is one of the important degrees of freedom in designing metasurfaces. When the metasurface units (i.e., supermolecules) are closely spaced, their strong inter-supermolecule interactions allow long-range interactions within the metasurface, significantly altering the energy signature spectrum of the system.[93] Micrometer-scale coherence length has been reported on disordered metal surfaces of certain permeability.[94]

Although the scales of the units of metallic metasurface nanostructures are much smaller than the wavelength of the incident continuous light, the dependence on the strong interactions and energy exchange between the units makes coherent control still possible. The interactions ensure that the excitation outside the half-wavelength has a sizable contribution to the target spot. Thus, the wavefront phase degrees of freedom limited by the diffraction limit can be used for selective excitation and control of hotspots in metallic metasurface structures with strong interaction between the units.

Consider monochromatic continuous light with shaped wavefront phase and amplitude incident on a metasurface with small spatial distances between elements and thus strong interactions. The excitations in the supramolecule can be theoretically regarded as point dipoles. The dipole–dipole interactions allow the energy to be coupled into the neighboring supramolecule to form a collective oscillation mode.[95] Based on coherent control, the collective oscillatory modes excited at different spatial locations are coherently phased at the desired locations. By controlling the phase and amplitude of the incident light wavefront, it is possible to realize the selective excitation of hotspots.

Wavefront shaping applied to subwavelength hotspot creation and movement was first theoretically proposed in dielectric periodic structures. A time-inversion method (or phase conjugation of monochromatic light) was used to generate a shaped wavefront to achieve subwavelength focusing at any selected point on the substrate.[97] Selective excitation of hotspots through spatial phase-shape beam control using higher-order beams such as Hermite–Gaussian and Laguerre–Gaussian beams was also experimentally achieved.[27]

Kao *et al.*[95] presented a theoretical concept for the generation and localization of subwavelength-level hotspots on two-dimensional arrays of nanoscale supramolecules using a coherent monochromatic beam. By depicting such metasurfaces as regular arrays of discretely interacting simple dipole scatterers, numerical calculations show that the energy can be almost exclusively focused on the subwavelength hotspot $(0.06\lambda \times 0.17\lambda)$ of an isolated supramolecule by tuning the spatial phase distribution of the incident beam alone. The generation and movement of the subwavelength hotspot $(0.22\lambda \times 0.17\lambda)$ are subsequently experimentally verified.[96]

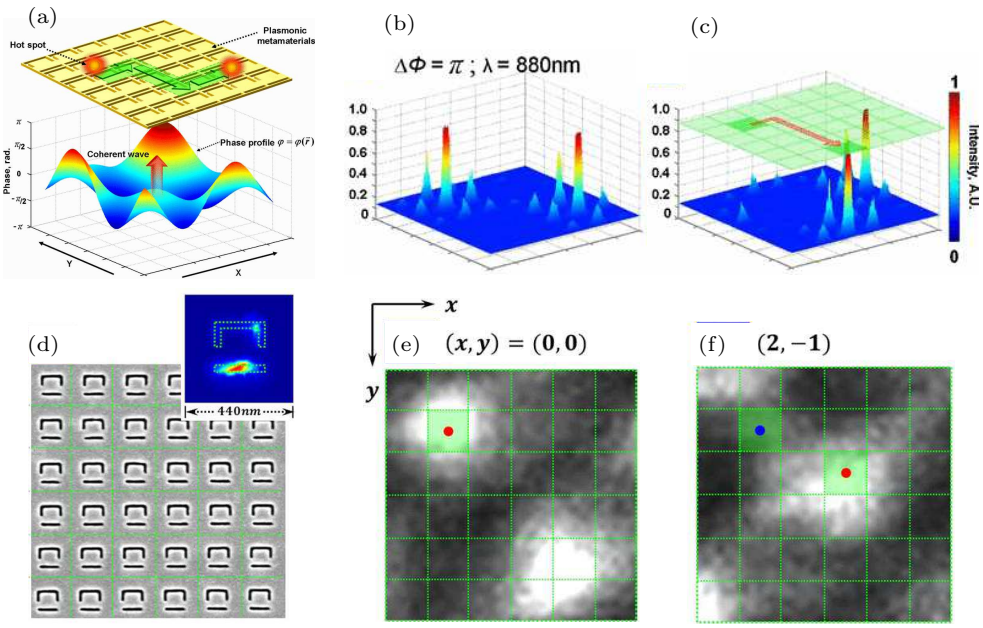


Fig. 4. Subwavelength continuum shift of metasurface hotspot realized by wavefront shaping. (a)–(c) Theory.[95] (a) Schematic diagram of the principle. (b) and (c) The metamaterial is modeled as an array of dipole scatterers, and the numerical simulation results demonstrate the feasibility of continuously moving the hotspot to a specified location by changing the phase distribution of the incident beam. (d)–(f) Experiment.[96] (d) SEM images of the metasurface. (e) and (f) Experimental realization of moving the hotspot continuously to a specified position by modulating the phase distribution of the incident beam.

4. Plasmon-enhanced spectroscopy combined with SLM

The highly localized light-field energy properties of SPs, including SPP and LSP hotspots, can significantly amplify the spectral signals generated by the interaction of light and matter. The surprising enhancement of the Raman signal, the first discovery of SERS, was observed in 1974 by Fleischman *et al.*[15] They found that electrochemically roughened silver electrodes play an important role in enhancing the Raman signal of pyridine molecules. This discovery greatly promotes further studies on the electromagnetic nature of plasmon-enhanced spectroscopy. Metal nanostructures capable of Raman enhancement and a broader type of SP-induced spectral enhancement were discussed and proved soon.[6] Inspired by the SERS phenomenon, Glass *et al.*[98] observed fluorescence enhancement of dye molecules, which were adsorbed on rough silver island films. And Chen *et al.*[99] reported second-harmonic enhancement on rough silver surfaces. The influence and applications of SP spectral enhancement are immense, extending into physics, chemistry, archaeology, biological sciences, pharmaceutical research, forensic science, etc. By incorporating the active control and selective excitation capabilities of SLM on SP modes, the applications in these fields will be further broadened.

4.1. SERS

Surface-enhanced Raman scattering is a highly sensitive method for exploring material and structural properties.[13,100] The inelastic scattering of light induced by molecular vibrations, i.e., the Raman scattering signal, is very weak due to its tiny scattering cross-section. Combining a molecule with a hotspot of plasmon excitations enhances the Raman signal by as much as 14 orders of magnitude, which allows the Raman signal to be easily observed. One of the key mechanisms of SERS is the electromagnetic mechanism. The Raman intensity is positively correlated with the intensity of the local electric field of the plasmon, so the optimization of the field enhancement of the hotspots is essential for the further enhancement of SERS. The design of nanostructures and the activation of their hotspots to enhance the signal intensity are crucial aspects of SERS research. Hotspots of structures such as rough metal surfaces, metal particle island membranes, and fractal nanoparticle clusters have been investigated for SERS. Interstitial modes of nanoparticle dimer structures have been reported to generate single-molecule SERS signals afterward.

Modulating the incident light wavefront phase, amplitude, and other degrees of freedom can focus the optical field energy on the hotspot to enhance the local field. Moreover, more efficiently coupling the incident light energy into the target plasmon mode can be achieved by wavefront shaping. In addition, the incident light dynamically modulates the spatial location and mode distribution of hotspots, which will be conducive to the ability of subwavelength-resolved SERS. Using SLM to shape the wavefront of the incident light can optimize and modulate the local field of the hotspot. Thus, the SERS signal is further enhanced and dynamically modulated.

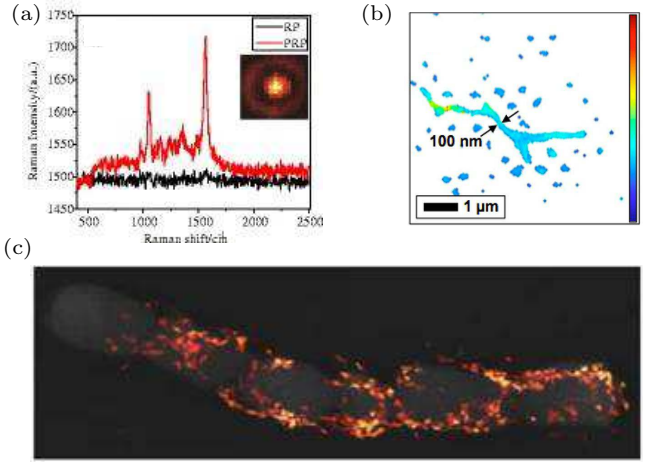


Fig. 5. (a) Comparison of SERS signals of silver nanosphere–thin silver film gap mode under excitation of a perfectly radially polarized beam (red) and radially polarized beam (black).[101] (b) Superresolution imaging of collagen fibers. Imaging results indicate that the thickness of collagen fibers is about 100 nm, which is consistent with measurements by other methods.[104] Super-resolution imaging of Escherichia coli.[105] Superimposition of both SERS super-resolution image (red) and SEM image (gray) of the bacterial sample.

Shaping the wavefront using SLM can optimize the excitation efficiency of specific LSP modes, thus improving the signal on top of the original SERS enhancement.[101–103] Yang *et al.*[101] utilized tightly focused, perfectly radially polarized light to improve the excitation efficiency of nanoparticle-thin-film interstitial modes and experimentally obtained SERS signals. In the tight-focusing scheme, irradiation of a perfectly radially polarized beam allows the incident light to enter at a resonant angle and form an SPP hotspot, effectively exciting the nanoparticle-thin-film interstitial modes located at the hotspot. This experiment generates perfectly radially polarized light through a helical plate and SLM modulation and tightly focuses it through a high numerical aperture oil-immersed lens. Their method enhances the SERS intensity of nanoparticle-thin-film interstitial structures by a factor of 20 compared to radially polarized light.

Precise positioning and subwavelength shifting of subwavelength hotspots allow simple implementation of subwavelength SERS imaging with far-field coherent control.[104–108] Thus, it avoids the problem of hotspots failing to illuminate part of the sample region under static illumination, which leads to imaging failures in certain regions. Combined with a customized super-resolution imaging scheme stochastic optical reconstruction microscopy (STORM) algorithm to observe and process the scintillation behavior of SERS hotspots, it can effectively utilize the sub-wavelength resolution of hotspots with the spectral resolution of Raman scattering. Ertsgaard *et al.*[104] combined STORM with SERS to achieve hotspot localization and super-resolution chemical imaging. This experiment utilized STORM to achieve super-resolution hotspot localization within 10 nm on an array of silver nanopores with dynamic adjustment of hotspot position. Based on the precise control of hotspot localization, this experiment also performed chemical imaging of collagen fibers, verifying the super-resolution imaging capability of the scheme.

4.2. Plasmon-enhanced photoluminescence

The phenomenon of photoluminescence (PL) refers to the spontaneous emission of a material, wherein it transitions to an excited electronic state after light excitation. This phenomenon finds extensive applications across various fields, from medical diagnostics to detection. Plasmon hotspots can significantly enhance fluorescence signals.[109] The fluorescent substances are strongly excited by the plasmon localized field of metal nanostructures to increase the excitation rate. At the same time, its emission properties are altered by the interaction with metal nanostructures, such as quantum yield, lifetime, and emission direction, which significantly enhances PL signals and radiation direction control. Like SERS, modulation of the incident optical degree of freedom can significantly optimize the local field strength and change the local field distribution of metal nanostructures, enabling optimization and dynamic modulation of plasmon-enhanced fluorescence.

Wavefront shaping of incident light can effectively excite specific nanostructured LSP modes and modulate their polarization, which is suitable for PL signal enhancement. Lee *et al.*[110] used adaptive optics algorithms to optimize the gold tip–surface gap mode to enhance PL signals of transition metal disulfides (TMDs). An adaptive algorithm was used to control the SLM to optimize the maximization of the in-plane component of the tip-LSP mode and to optimize the excitation of the in-plane dipole of the monolayer WSe_2 exciton. Experimentally, the PL of the WSe_2 monolayer was observed to be twice as strong as that of the conventional TEPL while maintaining a spatial resolution of 14 nm. Subsequently, the method was used to study the structural and optical response of nanoscale folds inherently formed in WSe_2 monolayers.[112]

The coupling of materials to metal nanostructures can be utilized, effectively converting the coherent control of the plasmonic exciton modes into the control of the material excitations. The spatial differences in the dipole moments of the different exciton modes of the material make the coupling strength of these exciton modes to the different discrete exciton modes of the metal nanostructures different. The exciton excitation ratios of the material can be modulated by changing the excitation of the discrete exciton modes. Koo *et al.*[111] realized the regulation of the intralaminar and interlaminar excitation ratios of the torsion heterogeneous bilayer of a transition-metal disulfide by dynamically manipulating discrete exciton modes of a gold nanocavity via shaped wavefront shaping. Based on this principle, the modulation of exciton excitation ratios is demonstrated for plasmon nanocavity-exciton

transistors. The dipole moments of the interlayer excitons of transition metal disulfides have an out-of-plane component, which is not present for the intralayer excitons. Therefore, different polarization modes of the nanocavity can be excited by adaptive algorithms to selectively achieve three states of enhanced intralayer excitons, enhanced interlayer excitons, or both. With this idea, a 2-bit all-optical transistor in an area of ~ 25 nm^2 is experimentally demonstrated.

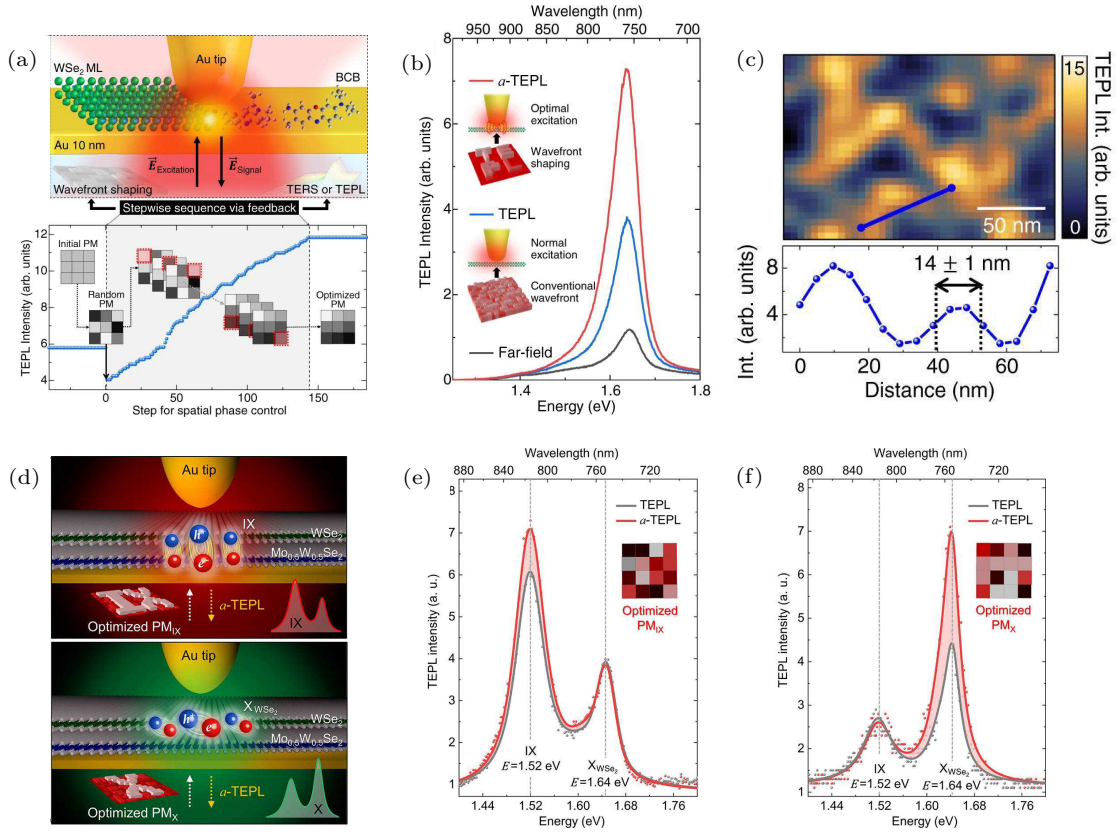


Fig. 6. (a)–(c) Adaptive tip-enhanced fluorescence spectra.[110] (a) Schematic of the experimental setup for tip-enhanced WSe_2 monolayer fluorescence with an adaptive optimization loop. (b) Comparison of far-field PL (black), TEPL spectra (blue), and adaptive-shaped wavefront TEPL spectra (red) for WSe_2 monolayers. (c) Adaptive TEPL image of Au film of monolayered WSe_2 (upper) with the blue line TEPL intensity distribution showing a spatial resolution of 14 nm (lower). (d)–(f) Selective control of intra-layer exciton vs. inter-layer exciton excitation.[111] (d) Schematic of the enhanced excitation of intra-layer exciton and inter-layer exciton tips for adaptive selective control of WSe_2 $Mo_{0.5}W_{0.5}Se_2$ heterobilayer. (e) Optimized interlayer exciton excitation. (f) Optimized intra-layer exciton excitation.

4.3. Plasmon-enhanced nonlinear signals

Optical nonlinearity arises from the superlinear interaction between matter and light. Under the electric dipole approximation, the nonlinear optical response of a material can be described by a power series expansion and results in mixing to generate new frequencies or modulate the original incident light propagation properties. In practical applications, the second harmonic generation (SHG) of second-order nonlinear processes, along with the third harmonic generation (THG) and four-wave mixing (FWM) of third-order nonlinear processes, has received much attention. Considering that the nonlinear coefficients of matter are usually small, a high-intensity light field is usually required. The plasmon localized light field can significantly enhance the nonlinear optical response of matter interacting with metal nanostructures.[113]

Optimization of SPP adiabatic focusing at the metallic tip by SLM pulse shaping is an effective countermeasure for controlling and enhancing its nonlinear signals. A study by Toma *et al.*[114] demonstrated the ability to optimize the SHG at the tip of a gold tip by utilizing an adaptive optimization algorithm. Experiments consisted of shaping femtosecond lasers by a pulse shaper of two SLMs, which were projected onto a conical gold SPP waveguide grating structure to generate an adiabatic focusing hotspot. Optimization of the SHG spectral peaks was achieved at three wavelengths. For each wavelength, they used an iterative optimization algorithm to change the third-order dispersion profile of the SPP pulse, demonstrating the manipulation and control of the wavefront at the tip of the gold. On the other hand, Kravtsov *et al.*[115] found that the gradient-field effect of the gold tip structure triggers an efficient third-order nonlinear response. Modulation by a $4f$ pulse shaper generates shaped pulses producing phase-uniform modes at the tip. In the near-IR spectral range (~ 800 nm), they demonstrated that when transitioning from

nondegenerate to degenerate FWM the conversion efficiency was up to 10^{-5}, and the corresponding third-order nonlinear optical susceptibility $\chi^{(3)}_{\mathrm{Au}}$ was up to 10^{-19} $\mathrm{m^2 \cdot V^{-2}}$. Based on this principle, they also realized femtosecond FWM nano-imaging of graphene, revealing its unique nonlinear nano-optical properties.[116]

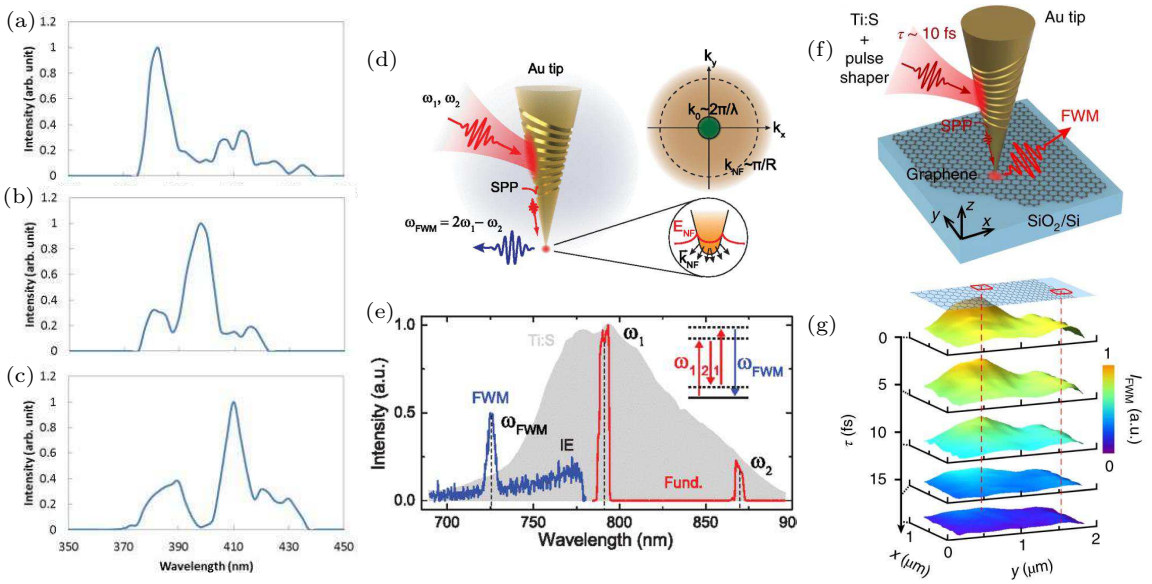


Fig. 7. (a)–(c) Second harmonic spectral control of a gold cone tip.[114] Second harmonic spectra were obtained by excitation of laser pulses with a third-order dispersion of 2000 fs^3 and inflection points of (a) 770 nm, (b) 800 nm, and (c) 830 nm, respectively. (d)–(e) Enhanced third-order optical nonlinearities driven by the field gradient at the gold conical tip.[115] (d) Schematic of the experimental setup and FWM signal generation principle. (e) Tip-generated FWM signal measurements are plotted with full laser spectrum (gray), fundamental wave scattering at the tip apex (red), incoherent emission (IE) background, and coherent FWM peak (blue). (f)–(g) Ultrafast FWM nano-imaging of graphene.[116] (f) Schematic diagram of the experimental setup. (g) FWM images of graphene with double-pulse excitation at different time delays.

5. Conclusion and perspectives

The powerful optical field-shaping capability of SLM for each degree of freedom of free-space light can be translated into the generation and modulation of SP modes of metal nanostructures. Through far-field optical control, SLM enables the excitation of plasmon modes with numerous tunable degrees of freedom for mode optimization and dynamic modulation. By shaping wavefront phase and amplitude for continuous light or shaping pulse for ultrashort pulses, it becomes possible to customize and modify almost any desired plasmon mode for a given nanostructure. Based on the design of excited SPP wavefronts, various specific SPP modes, such as SPP focusing, plasmon vortex beams, and plasmon diffraction-free beams, can be achieved and modulated. Based on coherently controlled excitation of LSP modes, selective excitation and subwavelength shifts of hotspots are demonstrated. The selective generation, optimization, and dynamic control of the plasmon modes are crucial for tailoring the desired modes for various applications, which are expected to play an important role in designing and developing nanophotonic signal transmission and signal processing devices.

The localized light field of surface plasmons significantly enhances the spectral signals generated by the interaction between light and matter. This allows for modulation of the plasmonic excitation modes, expanding the boundaries of applications in plasmon-enhanced spectroscopy. The combination with adaptive algorithms enables optimization of various plasmon-enhanced spectroscopy signals. Additionally, there are novel applications that combine nanoscale-resolution hotspots with spectral resolution. The various schemes combining plasmon-enhanced spectroscopy with SLM demonstrate the universality and expandability of structured light-optimized plasmon spectral enhancement. The tunable degrees of freedom offer promising research prospects.

Although many important studies support the critical role of the modulation supported by SLM in plasmon-enhanced spectroscopy applications, many other related areas of plasmon have yet to be explored in conjunction with structured light far-field dynamic control. Many exciting works have been reported so far. For example, holographic plasmonic nanotweezers have been demonstrated to trap and dynamically manipulate nanoparticles at subwavelength scales.[117] Surface plasmon microscopic sensing without any mechanical movement has been realized by shaping the wavefront profile, which greatly extends the utility of confocal-based SP sensing and imaging.[118] A novel ultrastable interferometer system with superior noise performance empowered by SLM shows promise for high-precision bioassay applications.[119] By using a spatial light modulator to arbitrarily control the location of hotspot excitation, arbitrarily dispersed microbubbles can be generated by the plasmon photothermal effect.[120] In ad-

dition to the field of plasmon photocatalysis, plasmon photoacoustics can also introduce the shaped light field for optimization and dynamic control. The combination of various structured light and shaped light fields with metal nanostructures promises exciting advances in the future, which will pave the way for further research on light–matter interactions and the development and design of nanophotonic devices.

Acknowledgments

Project supported by the Guangdong Major Project of Basic and Applied Basic Research (Grant No. 2020B0301030009), the National Key Research and Development Program of China (Grant No. 2022YFA1604304), and the National Natural Science Foundation of China (Grant No. 92250305).

References

[1] Barnes W L, Dereux A and Ebbesen T W 2003 *Nature* **424** 824
[2] Ozbay E 2006 *Science* **311** 189
[3] Maier S A 2007 *Plasmonics: fundamentals and applications* (New York: Springer)
[4] Schuller J A, Barnard E S, Cai W, Jun Y C, White J S and Brongersma M L 2010 *Nat. Mater.* **9** 193
[5] Yu H, Peng Y, Yang Y and Li Z Y 2019 *Npj Comput. Mater.* **5** 45
[6] Moskovits M 1985 *Rev. Mod. Phys.* **57** 783
[7] Wu H, Gao Y, Xu P, Guo X, Wang P, Dai D and Tong L 2019 *Adv. Opt. Mater.* **7** 1900334
[8] Zhan C, Chen X J, Yi J, Li J F, Wu D Y and Tian Z Q 2018 *Nat. Rev. Chem.* **2** 216
[9] Jain P K, Huang X, El-Sayed I H and El-Sayed M A 2007 *Plasmonics* **2** 107
[10] Homola J 2008 *Chem. Rev.* **108** 462
[11] Zhou X, Yang Y, Wang S and Liu X 2020 *Angew. Chem. Int. Ed.* **59** 1776
[12] Zhang X and Yang J 2019 *Front. Phys.* **7** 190
[13] Wang X, Huang S C, Hu S, Yan S and Ren B 2020 *Nat. Rev. Phys.* **2** 253
[14] Li J F, Li C Y and Aroca R F 2017 *Chem. Soc. Rev.* **46** 3962
[15] Fleischmann M, Hendra P J and McQuillan A J 1974 *Chem. Phys. Lett.* **26** 163
[16] Kneipp K, Wang Y, Kneipp H, Perelman L T, Itzkan I, Dasari R R and Feld M S 1997 *Phys. Rev. Lett.* **78** 1667
[17] Kinkhabwala A, Yu Z, Fan S, Avlasevich Y, Müllen K and Moerner W E 2009 *Nat. Photonics* **3** 654
[18] Wei F, Lu D, Shen H, Wan W, Ponsetto J L, Huang E and Liu Z 2014 *Nano Lett.* **14** 4634
[19] Chen H, Du L, Wu X, Zhu S, Yang Y, Fang H and Yuan X 2016 *Appl. Phys. Lett.* **109** 261904
[20] Kelly K L, Coronado E, Zhao L L and Schatz G C 2003 *J. Phys. Chem. B* **107** 668
[21] Rycenga M, Cobley C M, Zeng J, Li W, Moran C H, Zhang Q, Qin D and Xia Y 2011 *Chem. Rev.* **111** 3669
[22] Yu N and Capasso F 2014 *Nat. Mater.* **13** 139
[23] Singh A, Hugall J T, Calbris G and Van Hulst N F 2020 *ACS Photonics* **7** 2381
[24] Lin J, Mueller J P B, Wang Q, Yuan G, Antoniou N, Yuan X C and Capasso F 2013 *Science* **340** 331
[25] Awada C, Popescu T, Douillard L, Charra F, Perron A, Yockell-Lelièvre H, Baudrion A L, Adam P M and Bachelot R 2012 *J. Phys. Chem. C* **116** 14591
[26] Wan W, Gao J and Yang X 2016 *ACS Nano* **10** 10671
[27] Volpe G, Cherukulappurath S, Juanola Parramon R, Molina-Terriza G and Quidant R 2009 *Nano Lett.* **9** 3608
[28] Neff J A, Athale R A and Lee S H 1990 *Proc. IEEE* **78** 826
[29] Savage N 2009 *Nat. Photonics* **3** 170
[30] Zhang Z, You Z and Chu D 2014 *Light Sci. Appl.* **3** e213
[31] Chen P, Wei B, Hu W and Lu Y 2019 *Adv. Mater.* **32** 1903665
[32] Ren Y X, Lu R D and Gong L 2015 *Ann. Phys.* **527** 447
[33] Forbes A, Dudley A and McLaren M 2016 *Adv. Opt. Photonics* **8** 200
[34] Sato S 1979 *Jpn. J. Appl. Phys.* **18** 1679
[35] Ohtake Y, Ando T, Fukuchi N, Matsumoto N, Ito H and Hara T 2007 *Opt. Lett.* **32** 1411
[36] Matsumoto N, Ando T, Inoue T, Ohtake Y, Fukuchi N and Hara T 2008 *J. Opt. Soc. Am. A* **25** 1642
[37] Ren Y X, Li M, Huang K, Wu J G, Gao H F, Wang Z Q and Li Y M 2010 *Appl. Opt.* **49** 1838
[38] Lerner V, Shwa D, Drori Y and Katz N 2012 *Opt. Lett.* **37** 4826
[39] Mirhosseini M, Magaña-Loaiza O S, Chen C, Rodenburg B, Malik M and Boyd R W 2013 *Opt. Express* **21** 30196
[40] Čižmár T, Kollárová V, Tsampoula X, Gunn-Moore F, Sibbett W, Bouchal Z and Dholakia K 2008 *Opt. Express* **16** 14024
[41] Ring J D, Lindberg J, Mourka A, Mazilu M, Dholakia K and Dennis M R 2012 *Opt. Express* **20** 18955
[42] Gong L, Ren Y X, Xue G S, Wang Q C, Zhou J H, Zhong M C, Wang Z Q and Li Y M 2013 *Appl. Opt.* **52** 4566
[43] Wang X L, Ding J, Ni W J, Guo C S and Wang H T 2007 *Opt. Lett.* **32** 3549
[44] Gong L, Ren Y, Liu W, Wang M, Zhong M, Wang Z and Li Y 2014 *J. Appl. Phys.* **116** 183105
[45] Rosales-Guzmán C, Bhebhe N and Forbes A 2017 *Opt. Express* **25** 25697
[46] Okamoto T, Kamiyama T and Yamaguchi I 1993 *Opt. Lett.* **18** 1570
[47] Dienerowitz M, Gibson G, Dienerowitz F and Padgett M 2012 *J. Opt.* **14** 045003
[48] Brzobohatý O, Šiler M, Trojek J, Chvátal L, Karásek V, Paták A, Pokorná Z, Mika F and Zemánek P 2015 *Sci. Rep.* **5** 8106
[49] Andres-Arroyo A, Wang F, Toe W J and Reece P 2015 *Biomed. Opt. Express* **6** 3646
[50] Zayats A V, Smolyaninov I I and Maradudin A A 2005 *Phys. Rep.* **408** 131
[51] Fang Y and Sun M 2015 *Light Sci. Appl.* **4** e294
[52] Willets K A and Van Duyne R P 2007 *Annu. Rev. Phys. Chem.* **58** 267
[53] Zhao C and Zhang J 2011 *Appl. Phys. Lett.* **98** 211108
[54] Yuan G H, Wang Q, Tan P S, Lin J and Yuan X C 2012 *Nanotechnology* **23** 385204
[55] Gjonaj B, Aulbach J, Johnson P M, Mosk A P, Kuipers L and Lagendijk A 2011 *Nat. Photonics* **5** 360
[56] Wei S, Si G, Malek M, Earl S K, Du L, Kou S S, Yuan X and Lin J 2018 *Sci. Adv.* **4** eaao0533
[57] Choi W, Jo Y, Ahn J, Ahn J M, Seo E, Park Q H, Jhon Y M and Choi W 2017 *Nat. Commun.* **8** 14636
[58] Yuan G H, Yuan X C, Bu J, Tan P S and Wang Q 2011 *Opt. Express* **19** 224
[59] Gjonaj B, Aulbach J, Johnson P M, Mosk A P, Kuipers L and Lagendijk A 2012 *Nano Lett.* **12** 546
[60] Gjonaj B, Aulbach J, Johnson P M, Mosk A P, Kuipers L and Lagendijk A 2013 *Phys. Rev. Lett.* **110** 266804
[61] Seo E, Ahn J, Choi W, Lee H, Jhon Y M, Lee S and Choi W 2014 *Opt. Lett.* **39** 5838
[62] Dikken D J W, Korterik J P, Segerink F B, Herek J L and Prangsma J C 2016 *Sci. Rep.* **6** 25037
[63] Jo Y, Choi W, Seo E, Ahn J, Park Q H, Jhon Y M and Choi W 2017 *Sci. Rep.* **7** 9779
[64] Seo E, Jin Y H, Choi W, Jo Y, Lee S, Song K D, Ahn J, Park Q H, Kim M K and Choi W 2020 *Nat. Commun.* **11** 2575
[65] Padgett M J 2017 *Opt. Express* **25** 11265
[66] Genevet P, Lin J, Kats M A and Capasso F 2012 *Nat. Commun.* **3** 1278
[67] Chen J, Chen X, Li T and Zhu S 2018 *Laser Photonics Rev.* **12** 1700331
[68] Cho S W, Park J, Lee S Y, Kim H and Lee B 2012 *Opt. Express* **20** 10083
[69] Feng F, Si G, Min C, Yuan X and Somekh M 2020 *Light Sci. Appl.* **9** 95
[70] Durnin J, Miceli J J and Eberly J H 1987 *Phys. Rev. Lett.* **58** 1499
[71] Berry M V and Balazs N L 1979 *Am. J. Phys.* **47** 264
[72] Siviloglou G A and Christodoulides D N 2007 *Opt. Lett.* **32** 979
[73] Wang S, Zhang J, Fu M, He J and Li X 2021 *Nanomaterials* **11** 2941
[74] Zhang P, Wang S, Liu Y, Yin X, Lu C, Chen Z and Zhang X 2011 *Opt. Lett.* **36** 3191

[75] Lin J, Dellinger J, Genevet P, Cluzel B, De Fornel F and Capasso F 2012 *Phys. Rev. Lett.* **109** 093904
[76] Regan C J, Grave De Peralta L and Bernussi A A 2012 *J. Appl. Phys.* **112** 103107
[77] Salandrino A and Christodoulides D N 2010 *Opt. Lett.* **35** 2082
[78] Minovich A, Klein A E, Janunts N, Pertsch T, Neshev D N and Kivshar Y S 2011 *Phys. Rev. Lett.* **107** 116802
[79] Li L, Li T, Wang S M, Zhang C and Zhu S N 2011 *Phys. Rev. Lett.* **107** 126804
[80] Zuloaga J, Prodan E and Nordlander P 2009 *Nano Lett.* **9** 887
[81] Stockman M 1997 *Phys. Rev. E* **56** 6494
[82] Rabitz H, De Vivie-Riedle R, Motzkus M and Kompa K 2000 *Science* **288** 824
[83] Stockman M I 2013 *Nanoplasmonics: From Present into Future Plasmonics: Theory and Applications Challenges and Advances in Computational Chemistry and Physics* vol. 15, edn. Shahbazyan T V and Stockman M I (Dordrecht: Springer Netherlands) pp. 1–101
[84] Assion A, Baumert T, Bergt M, Brixner T, Kiefer B, Seyfried V, Strehle M and Gerber G 1998 *Science* **282** 919
[85] Bartels R, Backus S, Zeek E, Misoguti L, Vdovin G, Christov I P, Murnane M M and Kapteyn H C 2000 *Nature* **406** 164
[86] Dudovich N, Oron D and Silberberg Y 2002 *Nature* **418** 512
[87] Stockman M, Faleev S and Bergman D 2002 *Phys. Rev. Lett.* **88** 067402
[88] Aeschlimann M, Bauer M, Bayer D, Brixner T, García de Abajo F J, Pfeiffer W, Rohmer M, Spindler C and Steeb F 2007 *Nature* **446** 301
[89] Aeschlimann M, Brixner T, Cunovic S, Fischer A, Melchior P, Pfeiffer W, Rohmer M, Schneider C, Strüber C, Tuchscherer P and Voronine D V 2012 *IEEE J. Sel. Top. Quantum Electron.* **18** 275
[90] Aeschlimann M, Bauer M, Bayer D, Brixner T, Cunovic S, Fischer A, Melchior P, Pfeiffer W, Rohmer M, Schneider C, Strüber C, Tuchscherer P and Voronine D V 2012 *New J. Phys.* **14** 033030
[91] Brinks D, Castro-Lopez M, Hildner R and van Hulst N F 2013 *Proc. Natl. Acad. Sci. USA* **110** 18386
[92] Aeschlimann M, Bauer M, Bayer D, Brixner T, Cunovic S, Dimler F, Fischer A, Pfeiffer W, Rohmer M, Schneider C, Steeb F, Strüber C and Voronine D V 2010 *Proc. Natl. Acad. Sci. USA* **107** 5329
[93] Halas N J, Lal S, Chang W S, Link S and Nordlander P 2011 *Chem. Rev.* **111** 3913
[94] Bondareff P, Volpe G, Gigan S and Gresillon S 2015 *ACS Photonics* **2** 1658
[95] Kao T S, Jenkins S D, Ruostekoski J and Zheludev N I 2011 *Phys. Rev. Lett.* **106** 085501
[96] Kao T S, Rogers E T F, Ou J Y and Zheludev N I 2012 *Nano Lett.* **12** 2728
[97] Sentenac A and Chaumet P C 2008 *Phys. Rev. Lett.* **101** 013901
[98] Glass A M, Liao P F, Bergman J G and Olson D H 1980 *Opt. Lett.* **5** 368
[99] Chen C K, De Castro A R B and Shen Y R 1981 *Phys. Rev. Lett.* **46** 145
[100] Stiles P L, Dieringer J A, Shah N C and Van Duyne R P 2008 *Annu. Rev. Anal. Chem.* **1** 601
[101] Yang A, Du L, Dou X, Meng F, Zhang C, Min C, Lin J and Yuan X 2018 *Plasmonics* **13** 991
[102] Giuzio G, Martín Sabanés N and Domke K F 2020 *Appl. Spectrosc.* **74** 1407
[103] Shutova M, Sinyukov A M, Birmingham B, Zhang Z and Sokolov A V 2020 *Opt. Lett.* **45** 3709
[104] Ertsgaard C T, McKoskey R M, Rich I S and Lindquist N C 2014 *ACS Nano* **8** 10941
[105] Olson A P, Spies K B, Browning A C, Soneral P A G and Lindquist N C 2017 *Sci. Rep.* **7** 9135
[106] Olson A P, Ertsgaard C T, Elliott S N and Lindquist N C 2016 *ACS Photonics* **3** 329
[107] Tomita K, Kojima Y and Kannari F 2018 *Nano Lett.* **18** 1366
[108] Collard L, Pisano F, Zheng D, Balena A, Kashif M F, Pisanello M, D'Orazio A, De La Prida L M, Ciracì C, Grande M, De Vittorio M and Pisanello F 2022 *Small* **18** 2200975
[109] Fort E and Grésillon S 2008 *J. Phys. Appl. Phys.* **41** 013001
[110] Lee D Y, Park C, Choi J, Koo Y, Kang M, Jeong M S, Raschke M B and Park K D 2021 *Nat. Commun.* **12** 3465
[111] Koo Y, Lee H, Ivanova T, Savelev R S, Petrov M I, Kravtsov V and Park K D 2023 *ACS Nano* **17** 4854
[112] Koo Y, Kim Y, Choi S H, Lee H, Choi J, Lee D Y, Kang M, Lee H S, Kim K K, Lee G and Park K 2021 *Adv. Mater.* **33** 2008234
[113] Kauranen M and Zayats A V 2012 *Nat. Photonics* **6** 737
[114] Toma K, Masaki Y, Kusaba M, Hirosawa K and Kannari F 2015 *J. Appl. Phys.* **118** 103102
[115] Kravtsov V, AlMutairi S, Ulbricht R, Kutayiah A R, Belyanin A and Raschke M B 2018 *Phys. Rev. Lett.* **120** 203903
[116] Jiang T, Kravtsov V, Tokman M, Belyanin A and Raschke M B 2019 *Nat. Nanotechnol.* **14** 838
[117] Huft P R, Kolbow J D, Thweatt J T and Lindquist N C 2017 *Nano Lett.* **17** 7920
[118] Zhang B, Pechprasarn S and Somekh M G 2012 *Opt. Express* **20** 28039
[119] Pechprasarn S, Zhang B, Albutt D, Zhang J and Somekh M 2014 *Light Sci. Appl.* **3** e187
[120] Ohannesian N, Li J, Misbah I, Zhao F and Shih W C 2020 *ACS Omega* **5** 32481